



**HAL**  
open science

## Springtime changes in snow chemistry lead to new insights into mercury methylation in the Arctic

Catherine Larose, A. Domergue, Martine de Angelis, Daniel Cossa, Bernard Averty, Nicolas Maruszczak, Nicolas Soumis, Dominique Schneider, Christophe P. Ferrari

### ► To cite this version:

Catherine Larose, A. Domergue, Martine de Angelis, Daniel Cossa, Bernard Averty, et al.. Springtime changes in snow chemistry lead to new insights into mercury methylation in the Arctic. *Geochimica et Cosmochimica Acta*, 2010, 74 (22), pp.6263-6275. 10.1016/j.gca.2010.08.043 . insu-00562243

**HAL Id: insu-00562243**

**<https://insu.hal.science/insu-00562243>**

Submitted on 11 Mar 2021

**HAL** is a multi-disciplinary open access archive for the deposit and dissemination of scientific research documents, whether they are published or not. The documents may come from teaching and research institutions in France or abroad, or from public or private research centers.

L'archive ouverte pluridisciplinaire **HAL**, est destinée au dépôt et à la diffusion de documents scientifiques de niveau recherche, publiés ou non, émanant des établissements d'enseignement et de recherche français ou étrangers, des laboratoires publics ou privés.

---

## Springtime changes in snow chemistry lead to new insights into mercury methylation in the Arctic

Catherine Larose<sup>a, b, c</sup>, Aurélien Dommergue<sup>a, \*</sup>, Martine De Angelis<sup>a</sup>, Daniel Cossa<sup>d</sup>, Bernard Averty<sup>e</sup>, Nicolas Maruszczak<sup>a</sup>, Nicolas Soumis<sup>a</sup>, Dominique Schneider<sup>b, c</sup> and Christophe Ferrari<sup>a</sup>

<sup>a</sup> Université Joseph Fourier – Grenoble 1/CNRS, LGGE, 54 rue Molière BP 56, F-38402 Saint Martin d'Hères, France

<sup>b</sup> Laboratoire Adaptation et Pathogénie des Microorganismes, Université Joseph Fourier Grenoble 1, BP 170, F-38042 Grenoble Cedex 9, France

<sup>c</sup> CNRS UMR 5163, France

<sup>d</sup> Ifremer, Centre de Méditerranée, BP 330, F-83507 La Seyne sur mer, France

<sup>e</sup> Ifremer, Centre de Nantes, BP 21105, F-44311 Nantes Cedex, France

\*: Corresponding author : Aurélien Dommergue, Tel.: +33 0 4 76 82 42 11; fax: +33 0 4 76 82 42 01, email address: [dommergue@lgge.obs.ujf-grenoble.fr](mailto:dommergue@lgge.obs.ujf-grenoble.fr)

---

### Abstract:

Seasonal snow is an active media and an important climate factor that governs nutrient transfer in Arctic ecosystems. Since the snow stores and transforms nutrients and contaminants, it is of crucial importance to gain a better understanding of the dynamics of contaminant cycling within the snowpack and its subsequent release to catchments via meltwater. Over the course of a two-month field study in the spring of 2008, we collected snow and meltwater samples from a seasonal snowpack in Ny-Ålesund, Norway (78°56'N, 11°52'E), which were analyzed for major inorganic ions and some organic acids, as well as total, dissolved, bioavailable mercury (THg, DHg, BioHg, respectively) and monomethylmercury (MMHg) species. We observe a seasonal gradient for ion concentrations, with surface samples becoming less concentrated as the season progressed. A significant negative correlation between BioHg and MMHg was observed in the snowpack. MMHg was positively and significantly correlated to methanesulfonate concentrations. Based on these results, we propose a new model for aerobic methylation of mercury involving species in the dimethylsulfoniopropionate cycle.

30

## 1. INTRODUCTION

31 For High Arctic ecosystems, snow is one of the most important climatic factors. Snow is an active  
32 media that transfers particulates and gases between the atmosphere and the landscape (Jones,  
33 1999). It is highly photochemically active with snowpack impurities photolyzed to release reactive  
34 trace gases into the boundary layer (Grannas et al., 2007a), and, given its high albedo, fresh snow  
35 reflects as much as 90% of incoming radiation (Hinkler et al., 2008). Snow affects both the length of  
36 the growing season and primary plant production by acting as a soil insulator as well as a water and  
37 nutrient reservoir (Kuhn, 2001; Edwards et al., 2007). Atmospheric scavenging and condensation  
38 largely determine snowpack chemistry and snowpacks accumulate particles, solutes and pollutants  
39 over winter and spring (Tranter et al., 1986; Loseto et al., 2004). Once deposited, they are subject to  
40 redistribution through a variety of processes such as melt–freeze events during the winter season  
41 (Johannessen and Henriksen, 1978) and snow metamorphism (Colbeck, 1989; Kuhn, 2001). The  
42 geometry of the pore space, vapor pressure gradients and wind pressure, in addition to the physical-  
43 chemical properties of the particles themselves can also impact redistribution (Colbeck, 1989; Kuhn,  
44 2001).

45 The Arctic is exposed to mercury (Hg), a toxic metal that can be transformed to methylmercury  
46 (MeHg), a potent neurotoxin that bioaccumulates in food webs (see review by Fitzgerald et al.  
47 (2007)), through long-range atmospheric transport. Although there are no direct anthropogenic Hg  
48 sources in the Arctic, high levels have been found in the livers and tissues of marine mammals and  
49 birds (Wagemann et al., 1998; Campbell et al., 2005) leading to increased exposure for Native  
50 Communities that depend on these resources (AMAP, 2009). The discovery of atmospheric mercury  
51 depletion events (AMDEs) in the Arctic (Schroeder et al., 1998) led to the hypothesis that these could  
52 be the major sources of Hg to Arctic ecosystems. During AMDEs, atmospheric elemental mercury is  
53 oxidized to divalent mercury through reactions with halogens such as bromine radicals (Lindberg et  
54 al., 2001; Ariya et al., 2002) and then deposited onto snow surfaces at levels 400-800 fold higher than

55 background in the course of a few hours (Lu et al., 2001; Dommergue et al., 2010). Recent reports  
56 suggest that some of this newly deposited Hg is bioavailable, i.e. able to cross biological membranes  
57 (Scott, 2001; Lindberg et al., 2002; ~~Larose et al., 2010~~), but its post-depositional fate remains unclear.  
58 Field experiments have shown that Hg can be both oxidized and reduced in the snowpack (Lalonde et  
59 al., 2002; Dommergue et al., 2003; Poulain et al., 2004) and there is an increasing consensus that  
60 most, but not necessarily all, of the deposited mercury is photo-reduced and reemitted back to the  
61 atmosphere (Poulain et al., 2004; Kirk et al., 2006; Dommergue et al., 2010).

62 In addition to the uncertainty regarding Hg sources to the Arctic, the mechanisms that produce  
63 MeHg in these cold environments are to date unresolved, although several pathways have been  
64 proposed. Methylation can occur both biotically and abiotically; biotic Hg methylation depends on  
65 microbial activity and the concentration of bioavailable mercury (BioHg) (Barkay et al., 1997),  
66 whereas abiotic methylation depends on the presence of methyl donors. These donors include small  
67 organic molecules (i.e. methyl iodide and dimethylsulfide or acetate (Hall et al., 1995; Celo et al.,  
68 2006; Hammerschmidt et al., 2007)) and larger organic components of dissolved organic matter such  
69 as fulvic and humic acids (Weber, 1993; Siciliano et al., 2005). Hence, the chemistry of the snowpack  
70 influences both Hg speciation and its transformation.

71 Since the snow stores and transforms atmospherically derived pollutants (Colbeck, 1981; Daly and  
72 Wania, 2004; Lei et al., 2004), a better understanding of the dynamics of contaminant cycling within  
73 the snowpack, and its subsequent release to catchments *via* meltwater would help evaluate  
74 ecotoxicological impacts. The timing and magnitude of a pulse exposure is especially important for  
75 aquatic ecosystems during spring when biological activity increasingly active (Loseto et al., 2004). The  
76 chemical concentrations at the initial stages of melt have been shown to be many times higher (3-7  
77 fold) than averages for the entire snowpack in field and laboratory experiments, a phenomenon  
78 referred to as ionic pulse (Johannessen and Henriksen, 1978; Colbeck, 1981; Kuhn, 2001). As the  
79 snow begins to melt, soluble ions are removed by the first stages of percolation (e.g. Tranter et al.,

80 1986), followed by the preferential elution of some ions before others (Eichler et al., 2001). Non-  
81 polar organic molecules are also found in meltwater, but are less easily entrained by percolating  
82 water due to their low solubility (Meyer et al., 2006). Insoluble particulate material can also be  
83 removed by percolation, but usually remains in the snow until the final stages of melting (Hodgkins,  
84 1998; Lyons et al., 2003; Meyer et al., 2006). During spring melt, these soluble and insoluble  
85 impurities are released to the environment in a few weeks and can impact the chemistry of  
86 snowmelt-fed ecosystems (Williams et al., 2009).

87 Here, we present chemical data from a seasonal Arctic snowpack sampled over a two-month period  
88 in the spring of 2008 in Ny-Ålesund, Norway. The focus of this research is the storage, transfer and  
89 subsequent release of solutes and mercury from the snowpack to snowmelt-fed ecosystems. We also  
90 explore possible interactions among the different chemical parameters that could potentially be  
91 involved in mercury methylation.

## 92 **2. MATERIAL AND METHODS**

### 93 **2.1 Field site**

94 The spring field study was carried out between April 16<sup>th</sup>, 2008 and June 8<sup>th</sup>, 2008 at Ny-Ålesund in  
95 the Spitsbergen Island of Svalbard, Norway (78°56'N, 11°52'E). The field site, a 50 m<sup>2</sup> perimeter with  
96 restricted access (to reduce contamination from human sources), is located along the south coast of  
97 the Kongsfjorden, which is oriented SE-NW and open to the sea on the west side (Figure 1). The  
98 Kongsfjorden was free of sea ice throughout the study.

### 99 **2.2 Sampling**

100 Surface snow samples were collected daily for Hg speciation. Twice a week, a shallow pit was dug  
101 and both surface and basal samples were collected for ion and mercury analyses. Samples for ion  
102 measurements were collected in sterile polycarbonate vials (acuvettes®) and stored at -20°C until  
103 analysis. For Hg analyses, snow was collected in acid-washed 250 mL glass Schott bottles (see

104 cleaning protocol outlined in Ferrari et al. (2000) for more details) and subsampled for dissolved and  
105 BioHg. Samples for MMHg were collected in 125 mL acid-washed Teflon coated low-density  
106 polyethylene bottles, and stored frozen until analysis. The bottles were hermetically sealed, double-  
107 wrapped in polyethylene bags, stored at -20°C, and transported frozen to the laboratory. Meltwater was  
108 collected in acid-washed 250 mL glass Schott bottles from streams that formed the 1<sup>st</sup> of June, 2008.  
109 In order to determine the spatial variability in mercury deposition, we sampled two snowpits  
110 integrating snow fall since the previous summer, the first on the Holtedahlfonna glacier (sample date  
111 30/04/08, N79°08.17, E13°16.12, 1173 m asl, 40 km from the Kongsfjorden fjord) and the second on  
112 the Kongsvegen glacier (sample date 19/05/08, N78°45.29, E13°20.20, 670 m asl, 40 km from the  
113 Kongsfjorden) (Figure 1). The Holtedahlfonna pit, with a depth of 1.80 m, was sampled at 20 cm  
114 intervals, whereas the Kongsvegen pit, with a depth of 2.75 m, was sampled at 30 cm intervals.  
115 Field blanks were collected, filled with ultrapure water in the laboratory, opened during sample  
116 collection, and handled as samples. To avoid contamination, Tyvex® body suits and latex gloves were  
117 worn during sampling and gloves were worn during all subsequent handling of samples.

118

## 119 **2.3 Chemical analyses**

### 120 *2.3.1. Total Hg & speciation*

121 Total Hg (THg) in snow samples was measured in the field with a Tekran model 2600 using USEPA  
122 method 1631 revision E. Samples were oxidized with 0.5% v/v BrCl to preserve divalent Hg (Hg(II)) in  
123 solution and to digest strongly bound Hg(II) complexes. Excess BrCl was neutralized with pre-purified  
124 hydroxylamine hydrochloride. The sample was then automatically injected, together with SnCl<sub>2</sub>, into  
125 a reaction vessel, reducing Hg(II) to gaseous elemental Hg (Hg<sup>0</sup>). Hg<sup>0</sup> was carried in an argon stream  
126 to two online gold traps. After thermal desorption, Hg<sup>0</sup> was detected by atomic fluorescence  
127 spectrometry. The Tekran Model 2600 was calibrated every day with the NIST SRM-3133 Hg

128 standard. The limit of detection, calculated as 10 times the standard deviation of a set of 10 blanks,  
129 was  $0.3 \text{ ng.L}^{-1}$  and relative accuracy was determined as  $\pm 8\%$  using a certified reference material  
130 (ORMS-4, National Research Council Canada). All samples were analyzed in triplicate. Dissolved total  
131 Hg (DHg) concentrations were determined in all samples by measuring Hg concentrations after  
132 filtration on a  $0.45 \text{ }\mu\text{m}$  nylon filter (25 mm diameter, Cole-Parmer). Bioavailable Hg (BioHg)  
133 concentrations were determined using ~~the biosensor described in Larose et al. (2010)~~. BioHg is  
134 defined as the fraction of Hg able to enter cells. BioHg is detected using a genetically modified  
135 bacterium containing mercury resistance and luminescence genes, such that photons are produced  
136 in a dose dependent manner upon Hg exposure. Briefly, the biosensor was cultured overnight in LB  
137 medium containing  $100 \text{ }\mu\text{g.mL}^{-1}$  ampicillin at  $37^\circ\text{C}$  without agitation. The culture was resuspended in  
138 LB media and experiments were carried out using cells in mid-exponential growth phase ( $\text{OD}_{600}$  of  
139 0.4). Cells were exposed to either a series of Hg dilutions in order to obtain a standard curve, or to  
140 melted snow samples with unknown bioavailable Hg concentrations in a v/v ratio (sample volume  
141 added is equal to the volume of the biosensor solution) and incubated for two hours at  $37^\circ\text{C}$  without  
142 agitation. The Hg standards were prepared from serial dilutions of a  $\text{Hg}^{2+}$  solution (SRM-3133 Hg  
143 standard). Samples were analyzed in triplicate, with three independent cultures, and light emission  
144 was recorded using a Modulus luminometer. Luminescence was expressed as relative light units  
145 (RLU) and normalized for optical density.

146

### 147 *2.3.2. Monomethylmercury analysis*

148 MMHg was measured on unfiltered samples as volatile methyl mercury hydride, by purge and cryo-  
149 trapping gas chromatography, and detected as elemental Hg vapor by atomic fluorescence  
150 spectrometry (Tekran, Model 2500). The mercury hydrides (from methyl and inorganic mercury)  
151 were synthesized in the presence of  $\text{NaBH}_4$ , purged from the sample with He, concentrated and then  
152 separated by cryogenic chromatography before being converted into  $\text{Hg}^0$  in a furnace ( $800^\circ\text{C}$ ) and

153 detected by the AFS detector. This protocol is derived from the hydride generation technique  
154 described by Tseng et al. (1998) and improved by Stoichev et al. (2004). The hydrides are formed  
155 within a glass reactor and the column used is a silanized glass tube filled with Chromosorb W/AW-  
156 DMCS impregnated with 15% OV-3. Analytical reproducibility varied with time between 6% and 15%.  
157 Calibration was performed using dilutions of a  $1 \text{ g.L}^{-1}$  stock MMHg solution in isopropanol into an  
158 aqueous HCl (0.4% Suprapur, Merck) solution. In addition, we used certified reference material, the  
159 ERM-AE670 from the Institute for Reference Materials and Measurements (IRMM, European  
160 Commission), which is  $\text{CH}_3^{202}\text{HgCl}$  in a 2 % ethanol/water solution. The recovery of 0.05 and 0.1  
161  $\text{pmol.L}^{-1}$  of ERM-AE670 spikes in seawater samples was  $103 \pm 2\%$  and  $99 \pm 2\%$ , respectively. The  
162 MMHg measurements took place within two months of sampling.

163 In order to determine Hg speciation within the snowpack, Vimteq simulations (Visual MINTEQ), that  
164 include parameters such as chemical equilibrium, major ions, pH and some short chain organic  
165 compounds, were carried out.

166

### 167 2.3.3. Additional analysis

168 The pH of melted snow samples was measured at  $20^\circ\text{C}$  (Heito pH meter, Paris). The electrode was  
169 manually calibrated, prior to analysis, with three different pH buffers (pH 4, 7 and 10, Heito). The  
170 values were not corrected for *in situ* snow temperature. In order to examine possible interactions  
171 between Hg speciation and snow chemical composition, inorganic ions ( $\text{F}^-$  denoted FI,  $\text{NO}_3^-$ ,  $\text{Cl}^-$ ,  $\text{SO}_4^{2-}$ ,  
172  $\text{NH}_4^+$ ,  $\text{Ca}^{2+}$ ,  $\text{Na}^+$ ,  $\text{K}^+$  and  $\text{Mg}^{2+}$ ) and organic acid (methylsulfonic acid (MSA), glutaric acid (Glut), oxalic  
173 acid (Ox), acetate with a possible contribution of glycolate (Ace.Glyc), and formate) concentrations  
174 were measured at the Laboratoire de Glaciologie et Géophysique de l'Environnement by  
175 conductivity-suppressed Ion Chromatography using a Dionex ICS 3000. Due to the proximity of the  
176 fjord, leading to very high chloride and sodium concentrations, samples were diluted 10-fold for  
177 organic acids and minor ions and 100-1000 times for major ions prior to analysis.



## 178 **2.4 Statistics**

179

180 All data, with the exception of pH values, were log-transformed prior to statistical analysis in order to  
181 obtain data with a normal distribution. The transformation was successful for all data. Statistical data  
182 analysis was performed using JMP 5.1 software (SAS Institute, 2003) and R (The R Project for  
183 Statistical Computing <http://www.r-project.org>). Simple linear regression analysis was carried out to  
184 detect associations between the different chemicals. Principal component analysis (PCA) was  
185 performed to reduce the dimensionality of the data set using the ade4 data package for R. Samples  
186 were clustered using Ward's linkage for hierarchical cluster analysis, where the error sum of squares  
187 at each successive clustering step is minimized. Analysis of variance (ANOVA) and Tukey-Kramer HSD  
188 multiple comparison tests were then used to determine significant differences in chemical  
189 parameters among the different clusters in JMP 5.1. Statistical significance was set at a probability  
190 level  $\alpha < 0.05$ .

191

## **3. RESULTS**

### 192 **3.1 Snowpack dynamics**

193 The seasonal snowpack began to develop in October, 2007, but a rain event in January 2008 resulted  
194 in a decrease in snow depth and the formation of a relatively thick (~10 cm) ice layer above the soil  
195 surface. The snowpack reformed above the ice layer, had a thickness of about 40 cm at the beginning  
196 of the sampling period (16<sup>th</sup> of April), but had disappeared almost completely by the 8<sup>th</sup> of June.  
197 Snow melt began mid-May (around the 20<sup>th</sup>) and meltwater rivers that flowed to the fjord formed on  
198 the 1<sup>st</sup> of June, 2008. A total of 7 snowfall events occurred throughout the field season.

### 199 **3.2 Snowpack and meltwater chemistry**

200 The snowpack is strongly influenced by marine aerosols due to the proximity of the fjord, although  
201 continental sources possibly contribute to Na<sup>+</sup> and Mg<sup>2+</sup> concentrations. The dominant cations in the

202 snowpack were  $\text{Na}^+$  ( $1861 \mu\text{mol.L}^{-1}$ ) followed by  $\text{Mg}^{2+}$  ( $426 \mu\text{mol.L}^{-1}$ ) and  $\text{Ca}^{2+}$  ( $110 \mu\text{mol.L}^{-1}$ ), while  
203 the dominant anions were  $\text{Cl}^-$  ( $2119 \mu\text{mol.L}^{-1}$ ) followed by  $\text{SO}_4^{2-}$  ( $159 \mu\text{mol.L}^{-1}$ ) and  $\text{NO}_3^-$  ( $5 \mu\text{mol.L}^{-1}$ ).  
204 In meltwater, the average concentrations for cations and anions were 433, 263 and  $359 \mu\text{mol.L}^{-1}$  for  
205  $\text{Na}^+$ ,  $\text{Mg}^{2+}$ ,  $\text{Ca}^{2+}$ , respectively, and  $569 \mu\text{mol.L}^{-1}$  for  $\text{Cl}^-$ ,  $90 \mu\text{mol.L}^{-1}$  for  $\text{SO}_4^{2-}$  and  $4 \mu\text{mol.L}^{-1}$  for  $\text{NO}_3^-$   
206 (Entire data ranges are given in Supplementary material Table I). In the snowpack, pH ranged from  
207 acidic to circumneutral values (4 to 6.6) and was stable at a pH around 6.8 in meltwater.

208 Based on the Vimteq results, mercury chloride ( $\text{HgCl}_2$ ) is the dominant form of Hg complexes in all  
209 our samples, followed by  $\text{HgBrCl}$ ,  $\text{HgCl}_3^-$ ,  $\text{HgBr}_2$ . The speciation of Hg is driven by the large chloride  
210 concentrations, but remains uncertain due to the lack of knowledge on binding constants of mercury  
211 with organic matter and the lack of robust speciation data of organic matter in snow. The presence of  
212 Hg complexes bound to organic compounds could readily change the photoreactivity and  
213 bioavailability of these complexes.

214 We performed PCA analysis and then clustered the samples using Ward's linkage. The clustering  
215 results are presented in Table I and the PCA is presented in Figure 2. Seasonality is apparent, since  
216 Group 1 comprises early season surface samples and most of the basal samples, Group 2 contains  
217 mid-season surface samples, Group 3 contains late-season surface samples, and Group 4 is  
218 composed of meltwater samples. Although precipitation events occurred at different times  
219 throughout the field season, they had no effect on sample distribution within the PCA, since samples  
220 collected during snowfall events did not cluster together. In the graphical representation of the PCA  
221 analysis, the length of the arrow represents the relative importance of the associated parameter in  
222 determining the distribution of samples. Based on the PCA analysis carried out on our data, the most  
223 important parameters driving sample distribution are BioHg and THg (Group 1), MMHg, MSA and  
224 Glut (Group 2), inorganic ions (Group 5) and certain organic acids (Group 4). The clustering of  
225 samples in Group 3 is driven by low concentrations of inorganic ions and organic acids.

226 ANOVA and multiple comparison tests were carried out in order to determine significant differences  
227 in chemical parameters among the five groups derived through PCA analysis and clustering using  
228 Ward's linkage. The results of these comparisons are presented in Table I (Supplementary material).  
229 Chemical parameters varied significantly among groups, with the exception of THg, DHg and BioHg  
230 (data not shown) (Table I, Supplementary material). There appears to be a seasonal gradient, with  
231 early season snow (Group 1) that is generally more concentrated than snow sampled later in the  
232 season (Groups 2 and 3). Meltwater (Group 4) is enriched in ions relative to snow, with the exception  
233 of the five snow samples in Group 5 that had the highest mean  $\text{Na}^+$ ,  $\text{NH}_4^+$ ,  $\text{K}^+$ ,  $\text{Mg}^{2+}$ ,  $\text{Cl}^-$ ,  $\text{SO}_4^{2-}$  and  $\text{Br}^-$   
234 concentrations. Group 5 and Group 4 had the highest  $\text{Ca}^{2+}$  concentrations, and Group 4 had the  
235 highest levels of  $\text{NO}_2^-$  and organics.

236 Group 2 had the highest  $\text{NO}_3^-$  concentrations and Groups 2 and 4 had the highest MSA and glutaric  
237 acid levels. MSA and glutaric acid levels peaked in surface samples during May (Figure 3) and are  
238 significantly and positively correlated ( $r^2=0.62$ ,  $p=0.0013$ ,  $n=13$ ). There are no significant differences  
239 among the groups in terms of Na:Cl and Br:Cl ratios, and the mean values of these ratios are close to  
240 those of seawater (Na:Cl=0,855 and Br:Cl=0,0015). The meltwater group has significantly higher K:Cl  
241 and Mg:Cl ratios (0.052 and 0.474, respectively) than the other groups, for which the ratios are  
242 similar to seawater (K:Cl=0.0186 and Mg:Cl=0.193). Group 5 had the lowest Ca:Cl ratio, which is close  
243 to the seawater ratio (0.044), while the other groups had significantly higher values. The  $\text{SO}_4$ :Cl ratio  
244 was highest in Group 2 at 0.430, and was closest to the seawater ratio (0.103) in Groups 5 and 1.

245 Meltwater samples were collected as of the 1<sup>st</sup> of June. The first sample collected had the highest  
246  $\text{Na}^+$ ,  $\text{Cl}^-$ ,  $\text{K}^+$ ,  $\text{Mg}^{2+}$ ,  $\text{SO}_4^{2-}$  and MSA concentrations (Figure 4) and appears to correspond to the tail-end  
247 of the ionic pulse. Glutaric acid,  $\text{NO}_3^-$  and  $\text{NO}_2^-$  concentrations increased as melting progressed and  
248 no peak in  $\text{Br}^-$  and  $\text{NH}_4^+$  concentrations was observed. MMHg concentrations were highest in the first  
249 meltwater sample (1<sup>st</sup> of June), whereas concentrations of BioHg, DHg and THg peaked on the 2<sup>nd</sup>, 6<sup>th</sup>  
250 and 7<sup>th</sup> of June, respectively (Figure 4).

### 251 3.3 Hg dynamics

252 At the onset of sampling (April 16<sup>th</sup>, 2008), surface snow had high THg concentrations, with levels  
253 reaching almost 90 ng.L<sup>-1</sup>. These concentrations dropped to around 1 or 2 ng.L<sup>-1</sup> by the 9<sup>th</sup> of May and  
254 increased again just prior to melt. THg concentrations in basal snow were relatively low at the  
255 beginning of the sampling period and increased gradually to levels above those of the surface around  
256 the 9<sup>th</sup> of May. THg concentrations in both basal and surface snow increased slightly from the 17<sup>th</sup> to  
257 the 23<sup>rd</sup> of May (Figure 3). BioHg concentrations were higher in surface samples than basal samples  
258 and peaked at the beginning and end of the sampling period (Figure 3). No MMHg data for surface  
259 samples was available between April 16<sup>th</sup> and May 6<sup>th</sup> since THg concentrations were too elevated to  
260 allow the detection of the MMHg peak with our analytical setup, but as of May 9<sup>th</sup>, concentrations  
261 were around 0.045 ng.L<sup>-1</sup> and dropped progressively to about 0.010 ng.L<sup>-1</sup> by May 25<sup>th</sup>. Two large  
262 MMHg peaks were measured in surface snow on the 21<sup>th</sup> and 27<sup>th</sup> of May with concentrations  
263 reaching 0.299 and 0.511 ng.L<sup>-1</sup>, respectively. Basal snow MMHg levels were measured throughout  
264 the field period and concentrations were low, averaging 0.010 ng.L<sup>-1</sup>, with the exception of a peak  
265 (0.245 ng.L<sup>-1</sup>) on the 2<sup>nd</sup> of June (Figure 3).

266 Linear regression analysis was carried out to explore the relationship between different Hg species  
267 and the major parameters influencing sample distribution as determined by PCA analysis. No  
268 significant linear correlations were obtained between MMHg and SO<sub>4</sub><sup>2-</sup>, NO<sub>3</sub><sup>-</sup> or Cl<sup>-</sup> concentrations  
269 when samples were analyzed either together, by group or based on sampling depth. THg  
270 concentrations were correlated to Cl<sup>-</sup> concentrations in surface samples ( $r^2=0.31$ ,  $p=0.0032$ ,  $n=26$ )  
271 and basal samples ( $r^2=0.31$ ,  $p=0.039$ ,  $n=14$ ). Based on PCA analysis, MMHg and MSA concentrations  
272 are correlated, and both are anti-correlated to BioHg concentrations. MSA, MMHg and glutaric acid  
273 also appear to be correlated (Figure 2). Linear regression analysis was carried out to determine the  
274 significance of these relationships and MMHg and MSA are significantly, positively correlated  
275 ( $r^2=0.45$ ,  $p=0.0022$ ,  $n=18$ ), as are Glut and MSA ( $r^2=0.62$ ,  $p=0.0013$ ,  $n=13$ ), but there is no significant

276 linear relationship between MMHg and Glut ( $r^2=0.02$ ,  $p=0.70$ ,  $n=9$ ). MMHg and BioHg are  
277 significantly, negatively correlated in the snowpack ( $r^2=0.26$ ,  $p=0.0044$ ,  $n=26$ ), as are BioHg and MSA  
278 ( $r^2=0.52$ ,  $p=0.0018$ ,  $n=15$ ), while no significant relationship exists between BioHg and Glut ( $r^2=0.08$ ,  
279  $p=0.47$ ,  $n=8$ ).

280 THg and MMHg concentrations in glacier snowpits are presented in Figure 5. THg in both pits  
281 decreased rapidly with depth, with buried layers showing low or undetectable values. Both pits  
282 exhibit similar MMHg patterns with the highest concentrations at the surface, decreasing over the  
283 first 50 cm, then increasing to a peak at  $\sim 150$  cm, and decreasing below. In the Kongsvegen pit  
284 (Figure 5), unlike the Holtedahlfonna pit, MMHg levels increased again in the lowest part of the pit.  
285 Organics (MSA, glutaric acid) could only be detected in surface and bottom layers while  $SO_4:Cl$ ,  $Na:Cl$   
286 and  $Br:Cl$  ratios were similar to seawater.  $Mg:Cl$ ,  $K:Cl$  and  $Ca:Cl$  ratios were much higher than those of  
287 seawater. The detailed chemistry for both pits is given in Table II. No significant correlations were  
288 observed between MMHg and Hg, or between Hg species and ion concentrations.

## 289 **4. DISCUSSION**

### 290 **4.1 Snowpack and meltwater chemical composition**

291 The snowpack evolves chemically over time. We observe a seasonal gradient in ion concentrations in  
292 the snowpack, with the highest concentrations for most ions observed in early season surface and  
293 basal snow (Group 1), whereas the lowest concentrations were observed in samples collected in late  
294 spring, just prior to melt (Group 3). Melting can occur at air temperatures below  $0^\circ C$  when solar  
295 radiation is sufficiently intense and penetrates into the snowpack (Kuhn, 1987). As a result, the top  
296 snow layers melt first and the surface layers gradually become less concentrated in ions and particles  
297 as the season progresses. The photochemical reactivity of surface layers also contributes to changes  
298 in ion concentrations, with snowpack impurities photolyzed to release reactive trace gases such as

299 NO<sub>2</sub>, HONO, CH<sub>2</sub>O, BrO and Hg<sup>0</sup> to the boundary layer. These processes appear to be ubiquitous and  
300 their influence varies according to background radical concentrations (Grannas et al., 2007b).

301 Our results are consistent with those of Goto-Azuma et al. (1994) who observe higher ion  
302 concentrations at the base of an Arctic snowpack as a result of percolation and snowpack  
303 metamorphism. The surface and basal samples in Group 5 had the highest ion concentrations among  
304 all groups, including the meltwater group. This is surprising since meltwater mobilizes solutes and  
305 contaminants within the snowpack, thus becoming enriched relative to the snow (Kuhn, 2001; Meyer  
306 and Wania, 2008). The samples in Group 5 carry a strong marine salt signal, as determined by the  
307 different ion to Cl<sup>-</sup> ratios (Table I, Supplementary material). It is likely that the surface sample of this  
308 group (sample date 19/04/2009) contained sea-spray and was enriched by marine air masses. The  
309 signal of this event can later be traced in the basal samples following snowfall and elution. It is also  
310 possible that the highly concentrated basal samples consist of older snow that had undergone similar  
311 deposition events from marine air masses.

312 Mid-season surface snow samples (Group 2, May 9<sup>th</sup> to May 30<sup>th</sup>) had high levels of glutaric acid, MSA  
313 and NO<sub>3</sub><sup>-</sup>, in addition to the highest SO<sub>4</sub><sup>2-</sup> to Cl<sup>-</sup> ratio among all groups. Glutaric acid, a C<sub>5</sub> dicarboxylic  
314 acid commonly found in aerosols and as cloud-condensation nuclei, is derived from a variety of  
315 sources including anthropogenic emissions such as motor exhaust, as well as biogenic emissions from  
316 the ocean (Kawamura and Ikushima, 1993; Kawamura and Kasukabe, 1996). Senescent marine  
317 phytoplankton cells release lipidic cell components (chlorophyll, chlorophyll phytyl chain,  
318 carotenoids, sterols, and unsaturated fatty acids (oleic acid, alkenones and unsaturated alkenes)  
319 (Rontani, 2001) that can be photooxidized to shorter diacids. Among the diacids, oxalic acid is  
320 generally the most abundant in aerosols, followed by succinic, malonic and glutaric acid (Kawamura  
321 and Kasukabe, 1996). This has been observed in diverse environments worldwide, including the  
322 Arctic. Another pathway involved in diacid production is the reaction of O<sub>3</sub> with cyclohexene, a  
323 symmetrical alkene molecule (Rontani, 2001). Hence, diacids in the marine environment originate

324 from two major processes: long-range transport from industrialized continents and *in situ*  
325 photochemical production. Legrand et al. (2007) reported seasonal differences in diacid  
326 concentrations in aerosols of a coastal site, with high oxalic acid and low C<sub>5</sub> and C<sub>4</sub> concentrations in  
327 the winter. They proposed that ageing of air masses during transport favored the production of  
328 short-chain diacids through the successive oxidation of C<sub>5</sub> and C<sub>4</sub> diacids. This is consistent with our  
329 data, as the early season snow oxalic acid in the first sample of Group 5 seems to originate from  
330 older marine air masses that travelled over the Arctic Ocean (HYSPLIT air mass trajectory model, data  
331 not shown). Glutaric acid was almost undetectable at the beginning of the season, but  
332 concentrations were high in samples from Group 2 collected in surface snow during the month of  
333 May. In the summer, Legrand et al. (2007) reported peak concentrations of C<sub>5</sub> and C<sub>4</sub> acids in a mid-  
334 latitude marine atmosphere, which may be attributed to unsaturated fatty acid degradation. The  
335 high glutaric acid concentrations relative to oxalic acid in our data set suggest that fatty acids  
336 originated from proximal marine emissions as the succession of oxidations to shorter diacids did not  
337 lead to total C<sub>5</sub> and C<sub>4</sub> depletion. Glutaric acid is also significantly positively correlated to MSA, which  
338 further supports the presence of a close marine source of organic acids. MSA is a photo-oxidation  
339 product of DMS, which itself is a derivative of dimethylsulphoniopropionate (DMSP) produced by  
340 phytoplankton (Bentley and Chasteen, 2004). DMSP is known as both an osmoprotectant and  
341 cryoprotectant for microorganisms, as well as a carbon and sulfur source. It is released from  
342 senescent or stressed cells (Kiene et al., 2000). MSA has been shown to exhibit a distinct seasonality  
343 that is linked to biological activity in Arctic waters and the importance of the phytoplankton bloom to  
344 dimethylsulfate (DMS) concentrations has also been reported (Leck and Persson, 1996). The most  
345 recent published data available on algae blooms in Svalbard were collected in 2007 and show that  
346 the bloom occurred in May (Narcy et al., 2009). Although the data for the 2008 period are  
347 unavailable, it is likely that the bloom occurred at the same period of the year.

348 The chemical changes of a snowpack and runoff are influenced by the chemical composition of the  
349 snow and wintertime refreezing processes of the meltwater (Colbeck, 1981; Davies et al., 1982; Bales  
350 et al., 1993). The first flush of meltwater is usually highly concentrated, with the preferential elution  
351 of certain solutes over others leading to a pulse (Colbeck, 1981; Goto-Azuma et al., 1994). Meltwater  
352 samples had mean ion concentrations that were comparable to those reported for early seasonal  
353 snow (Group 1), with the exception of  $K^+$ ,  $Mg^{2+}$  and  $Ca^{2+}$  concentrations, which were much higher. In  
354 addition, the Mg:Cl, K:Cl and Ca:Cl were also significantly higher than in the early season samples.  
355 These elevated ratios may reflect the contact between the meltwater and the soil, since meltwater  
356 can be modified by soil processes due to infiltration and leaching (Williams et al., 2009) in addition to  
357 the flushing of soil pore fluids upon soil thaw. Although solute concentrations in the first meltwater  
358 sample are high, it is likely that the pulse occurred before the formation of meltwater rivers and that  
359 we only measured the tail-end of the pulse, since we were unable to detect preferential elution.  
360 Nevertheless, we did observe some fractionation of mercury species, as MMHg was preferentially  
361 eluted to BioHg, followed by the dissolved fraction. The chemical composition of the DHg fraction is  
362 unknown, but likely consists of different forms of Hg that are soluble, but not bioavailable. The  
363 remaining Hg was eluted last and was probably bound to insoluble particles (Figure 4).

364

#### 365 **4.2 Snowpack Hg dynamics**

366 While AMDEs have been shown to lead to high deposition of Hg onto snow surfaces, the post-  
367 depositional fate of Hg has yet to be completely clarified. The current consensus among researchers  
368 now is that a large portion is reemitted back to the atmosphere following an event (Poulain et al.,  
369 2004; Kirk et al., 2006; Dommergue et al., 2010). We recorded an AMDE at the beginning of the field  
370 season that led to high concentrations in the snowpack (max value  $90 \text{ ng.L}^{-1}$ ), but these decreased  
371 rapidly. At the beginning of the field season, basal snow sample Hg concentrations were low, around  
372  $1\text{-}2 \text{ ng.L}^{-1}$ , yet they increased almost 8-fold following the AMDE-induced peak in surface snow



373 concentrations. Although the transfer mechanisms that lead to this increase are unclear, Hg was  
374 likely transferred into deeper layers of the snowpack from the surface bound to particulate matter or  
375 as a mobile chemical form that percolated through the snowpack (Daly and Wania, 2004; Johnson et  
376 al., 2008). If the Hg levels in the basal layers of the snow result from AMDEs, then the quantity  
377 retained by the snowpack represents roughly 10% of the initial loading. These results suggest that  
378 although a large portion of Hg deposited by AMDEs returns to the atmosphere, a significant quantity  
379 is trapped within the snowpack, from which it can then be transferred to other systems upon  
380 melting.

381 In a review on Hg microbiogeochemistry in polar environments, Barkay and Poulain (2007) outline  
382 possible methylmercury sources and methylation pathways in arctic ecosystems. These include  
383 atmospheric and aquatic sources with either abiotic or biotic methylation pathways. In terms of  
384 snowpack MMHg concentrations, the most plausible sources are: 1) an atmospheric source of MMHg  
385 due to the photodegradation and deposition of plankton-derived dimethylmercury, 2) *in situ*  
386 methylation of BioHg in the snowpack (microbial), 3) biotic or abiotic methylation in the atmosphere,  
387 and 4) *in situ* phytoplankton MMHg production.

388 Based on a positive correlation between MMHg and chloride in snow collected from Ellesmere Island,  
389 Nunavut, Canada, St. Louis et al. (2005) suggested that MMHg was bound to seasalt aerosols (i.e.  
390 source 1). Constant et al. (2007) also reported a similar correlation in subarctic snow. This led to the  
391 hypothesis that MMHg originated from gaseous dimethylmercury (DMHg) formed by phytoplankton  
392 in the water column, whose production has been reported in Arctic waters (Kirk et al., 2008). Since  
393 DMHg is highly volatile, it can be emitted from the seawater and be oxidized to MMHg in the  
394 atmosphere by free radical species such as  $\text{OH}^\bullet$  and  $\text{Cl}^\bullet$  (Niki et al., 1983a; Niki et al., 1983b) before  
395 being deposited onto nearby snow surfaces (St. Louis et al., 2005). However, no correlation between  
396 MMHg and chloride was observed in our data set, even when the different snow types and groups  
397 are analyzed individually. St Louis et al. (2007) also observed a lack of correlation between MMHg

398 and chloride, but still attributed MMHg concentrations to DMHg production and subsequent  
399 photodegradation based on the proximity of their sampling sites to the water.

400 MMHg is significantly anti-correlated to BioHg in our snow samples, which could suggest that a  
401 fraction of the BioHg is efficiently scavenged to form MMHg. Bacteria have been isolated from Arctic  
402 snowpacks (Amato et al., 2007) and microbial activity has been measured at temperatures down to -  
403 20°C (Christner, 2002). Poulain et al. (2007) reported the presence of Hg resistance (*merA*) gene  
404 transcripts in Arctic biofilm samples and, hence, it is likely that the microbial populations in Arctic  
405 environments are able to metabolize mercury. Whether Hg methylation can occur in the snow  
406 remains uncertain. Constant et al. (2007) reported increases in the MMHg:THg ratio that were  
407 positively correlated with bacterial colony counts and particles. These results led to the hypothesis  
408 that MMHg was being formed within the snowpack, despite the absence of correlation with sulfate-  
409 reducing bacteria (SRB), the principal methylators in anoxic environments. Since the snowpack is  
410 most likely oxygenated, other species capable of methylating Hg aerobically may exist.

411 Hg methylation has been linked to sulfur and iron metabolism in bacteria (Fleming et al., 2006; Kerin  
412 et al., 2006). Early research into the mechanisms of Hg methylation was based on anoxic sediments  
413 (Compeau and Bartha, 1985; Berman et al., 1990) and quickly focused on anaerobic, sulfate reducing  
414 bacteria. Choi et al. (1994) used radio-labeled <sup>14</sup>C incorporation and enzyme activity measurements  
415 to propose that methylation involves the tetrahydrofolate (THF) pathway in *Desulfovibrio*  
416 *desulfuricans*. In their model, the methyl group is transferred from CH<sub>3</sub>-tetrahydrofolate via  
417 methylcobalamin with either serine or formate as the original methyl donors during the acetyl-CoA  
418 synthase pathway.

419 In our samples, MMHg is positively correlated to MSA, a by-product of DMSP and an important  
420 molecule in the marine microbial sulfur cycle (Kiene et al., 2000). DMSP can be metabolized *via*  
421 several different pathways in the water column (Figure 6), one involving enzymatic cleavage to  
422 produce DMS, but also by demethylation and demethiolation to produce methylsulfate in bacterial

423 cells. Methylsulfate can then undergo thiol transmethylation to produce DMS (Bentley and Chasteen,  
424 2004). The initial demethylation (and a possible second demethylation) has recently been shown to  
425 be THF-dependent and catalyzed by an amino-methyltransferase enzyme in aerobic bacteria (Reisch  
426 et al., 2008). The similarities to anaerobic Hg methylation are striking, and it is possible that a fraction  
427 of BioHg, upon entering the cell, undergoes methylation by aerobic bacteria that are able to  
428 demethylate or metabolize DMSP. A total of four methyl transfer reactions occur at various stages of  
429 DMSP metabolism, and BioHg may serve as a methyl group acceptor at some point in the process.  
430 BioHg is also negatively correlated to MSA, which further suggests DMSP implication (or the  
431 implication of another product of DMSP metabolism) in the methylation of Hg. This is compounded  
432 by the fact that neither MMHg nor BioHg concentrations are significantly correlated to glutaric acid,  
433 a biogenically produced dicarboxylic acid. Finally, this hypothesis is reinforced by recent results  
434 demonstrating Hg methylation in the oxic oceanic water column (Monperrus et al., 2007; Cossa et al.,  
435 2009; Sunderland et al., 2009).

436 Whether methylation occurs within the snowpack, in the water column or both simultaneously  
437 remains under debate, but, methylation appears to require a substrate involved in DMSP cycling.  
438 Hence, coastal sites may be especially at risk for MMHg contamination, since they are reported to  
439 contain higher Hg concentrations than inland sites (Douglas and Sturm, 2004; Brooks et al., 2008) and  
440 are close to a DMSP source. In addition, the run-off during springtime melt may return concentrated  
441 water back to the aquatic ecosystem.

442 Although the case for biologically-produced MMHg is strong, the data from the snow pits sampled on  
443 April 30<sup>th</sup> and May 19<sup>th</sup> point to a combination of sources for MMHg in remote areas. Since the fjord  
444 is 40 km away from both sampling sites, its effect on the chemical composition of snow is less  
445 important, as reflected by the 1-3 order of magnitude lower Na<sup>+</sup> and Cl<sup>-</sup> concentrations measured in  
446 our pit samples. MMHg concentrations were generally higher than in the surface waters of the fjord  
447 (seasonal average  $10 \pm 4 \text{ pg.L}^{-1}$ ) and higher than average MMHg levels in the seasonal snowpack,

448 excluding the peaks measured towards the end of May. In addition, BioHg and MSA concentrations  
449 were generally below detection limit in these samples, which would exclude the biotic methylation  
450 mechanism outlined above. THg levels were also low, and neither THg nor MMHg were significantly  
451 correlated to  $Cl^-$  concentrations. Taken together, these results suggest alternate sources for MMHg.  
452 Abiotic methylation may be occurring in the atmosphere and involve methyl donors such acetate and  
453 reactive mercury (not strongly bound) in the aqueous phase, as proposed by Hammerschmidt et al.  
454 (2007). Methylation kinetics obtained by Gardfeldt et al. (2003) suggest a reaction pathway where  
455 Hg(II) is bound to organic complexes. Nevertheless, this does not exclude an oceanic source for  
456 MMHg, since the layers with marine organics also exhibit the highest MMHg concentrations. Finally,  
457 the elevated levels of MMHg in the Kongsvegen basal layer may point to biotic methylation. Amato  
458 et al. (2007) found higher concentrations of bacteria in the summer layer in a pit dug on the same  
459 glacier and this may reflect microbial growth and metabolism. These potential sources of MMHg may  
460 have been masked at the coastal site by the influence of the fjord. It is likely that MMHg is supplied  
461 to Arctic environments by various pathways that are occurring simultaneously.

462

#### 463 **Acknowledgements**

464 This work is funded by EC2CO, LEFE-CHAT and by the French Polar Institute IPEV for logistical support  
465 (program CHIMERPOL). We acknowledge Alan Le Tressoler and AWIPEV for field support, as well as  
466 Emmanuel Prestat for advice on statistics and I. Moreno and J. Cozic for their help in the laboratory.  
467 We would also like to thank M. Legrand for the scientific discussions. CL would like to acknowledge  
468 the FQRNT (le Fond Québécois de la Recherche sur la Nature et les Technologies) for a PhD research  
469 fellowship.

470

471

472 Table I: Groups, corresponding samples and sample dates as derived by PCA analysis and Ward's  
473 linkage for hierarchical clustering analysis

Cluster name	Nature of the sample	date	
Group 1	Early season surface snow and most of basal snow samples	16/04/08 to 06/05/2008	474 475 476
Group 2	Mid-season surface snow	09/05/2008 to 30/05/2008	477
Group 3	Late-season surface snow	01/06/2008 to 8/06/2008	
Group 4	Meltwater samples	01/06/2008 to 08/06/2008	478
Group 5	An early surface sample and four basal samples	19/04/2008, 23/04/2008, 29/04/2008, 09/05/2008, 20/05/2008	479 480

481

482

483

484

485 Table II: Measured species concentrations at different depths at the Holtedahlfonna (H) and  
 486 Kongsvegen (K) snowpits. Ion concentrations are expressed in  $\mu\text{mol.L}^{-1}$ . Standard error was less than  
 487 10%.

488

Snow sample	MSA	Cl <sup>-</sup>	Br <sup>-</sup>	NO <sub>3</sub> <sup>-</sup>	Glut	SO <sub>4</sub> <sup>2-</sup>	Na <sup>+</sup>	NH <sub>4</sub> <sup>+</sup>	K <sup>+</sup>	Mg <sup>++</sup>	Ca <sup>++</sup>
H 0cm	0.12	5.6	0.00	1.3	0.03	5.4	5.4	1.6	0.13	1.8	1.8
H 20 cm	0.00	18.1	0.22	0.6	0.00	1.8	17.3	0.6	0.19	3.9	1.8
H 40 cm	0.00	62.4	0.52	3.1	0.00	8.4	56.8	2.2	0.89	16.3	4.8
H 60 cm	0.00	35.8	0.43	0.8	0.00	3.5	32.9	1.2	0.38	11.3	3.8
H 80 cm	0.00	46.2	0.43	0.7	0.00	4.7	37.8	1.1	0.37	12.6	2.7
H 100 cm	0.00	7.3	0.09	0.5	0.00	1.9	6.5	0.7	0.08	2.5	1.7
H 120 cm	0.00	22.0	0.22	0.7	0.00	2.1	19.4	1.3	0.29	6.4	1.9
H 140 cm	0.00	14.6	0.13	0.4	0.00	1.5	14.0	0.4	0.15	4.3	1.4
H 160 cm	0.00	0.9	0.00	0.4	0.00	0.6	0.8	0.5	0.03	0.3	0.9
H 180 cm	0.12	3.7	0.00	1.6	0.00	2.3	0.8	0.8	0.09	4.1	3.8
K 0 cm	1.66	13.5	0.22	3.1	0.07	16.1	12.0	4.7	0.11	5.9	4.7
K 30 cm	0.00	15.1	0.22	0.6	0.01	2.6	13.7	0.6	0.15	5.2	1.9
K 60 cm	0.00	39.0	0.30	2.0	0.00	5.7	38.4	1.0	0.35	11.7	3.3
K 90 cm	0.00	100.4	0.90	1.0	0.00	10.8	85.7	1.0	1.37	28.1	6.4
K 120 cm	0.00	34.2	0.34	1.1	0.00	3.2	34.7	0.4	0.40	10.3	2.1
K 150 cm	0.00	21.3	0.22	0.9	0.00	4.4	19.9	1.0	0.26	6.7	2.5
K 180 cm	0.00	46.4	0.47	0.5	0.00	5.3	40.5	1.3	0.45	17.0	3.3
K 210 cm	0.00	25.9	0.30	0.9	0.01	3.6	25.5	1.2	0.35	9.1	4.6
K 240 cm	0.10	12.0	0.13	0.5	0.03	3.6	12.2	0.9	0.17	5.7	3.3
K 270 cm	0.02	6.9	0.13	0.1	0.00	0.4	5.4	0.5	0.10	1.3	0.6

489

490

491

492  
493  
494  
495  
496  
497  
498  
499  
500  
501  
502  
503  
504  
505  
506  
507  
508  
509  
510  
511  
512  
513  
514  
515  
516  
517  
518  
519

#### FIGURE CAPTION

Figure 1: Map of the study area. Left map: Location of the Svalbard Archipelago. Right map: Ny-Ålesund (black star), Svalbard (Norway) and its surroundings. Sampling sites on the glaciers are shown with black triangles.

Figure 2: Principal component analysis for the sampling period. Chemical data ( $\mu\text{mol.L}^{-1}$  or  $\text{ng.L}^{-1}$  for Hg species) were log-transformed prior to analysis. The data set covers the entire sampling period (16<sup>th</sup> April- June 8<sup>th</sup>). Abbreviations: Glut=glutaric acid, MSA=methanesulfonic acid, Ox=oxalic acid, For=formate, F=fluoride, Ace.Glyc=acetate-glycolate, BioHg=bioavailable Hg, THg=total Hg, MeHg=monomethylmercury, DHg=dissolved total Hg

Figure 3: Chemical profiles over time for organics (MSA, glutaric acid, oxalic acid) and different mercury species. Organic concentrations are expressed in  $\mu\text{mol.L}^{-1}$ , total mercury (THg) and bioavailable mercury (BioHg) are expressed in  $\text{ng.L}^{-1}$ . Monomethylmercury (MMHg) concentrations are expressed in  $\text{pg.L}^{-1}$ . Full squares represent surface samples, open squares represent basal samples and crosses are meltwater samples. Surface samples for MMHg and HgT are presented on a log-scale. All analyses were carried out in duplicate or triplicate and standard error was less than 10%.

Figure 4: Meltwater elution curves for major ions and different mercury species over time. Ion concentrations are expressed in  $\mu\text{mol.L}^{-1}$ , total (THg), dissolved total (DHg) and bioavailable (BioHg) mercury concentrations are expressed in  $\text{ng.L}^{-1}$ . Monomethylmercury (MMHg) concentrations are in  $\text{pg.L}^{-1}$ . Analyses were carried out in duplicate or triplicate and standard error was less than 10%.

520 Figure 5: Snowpit total mercury (THg) and monomethylmercury (MMHg) profiles for Høltedahlfonna  
521 (sample date 30/04/2008) and Kongsvegen (sample date 19/05/2008) glaciers. ▲

522

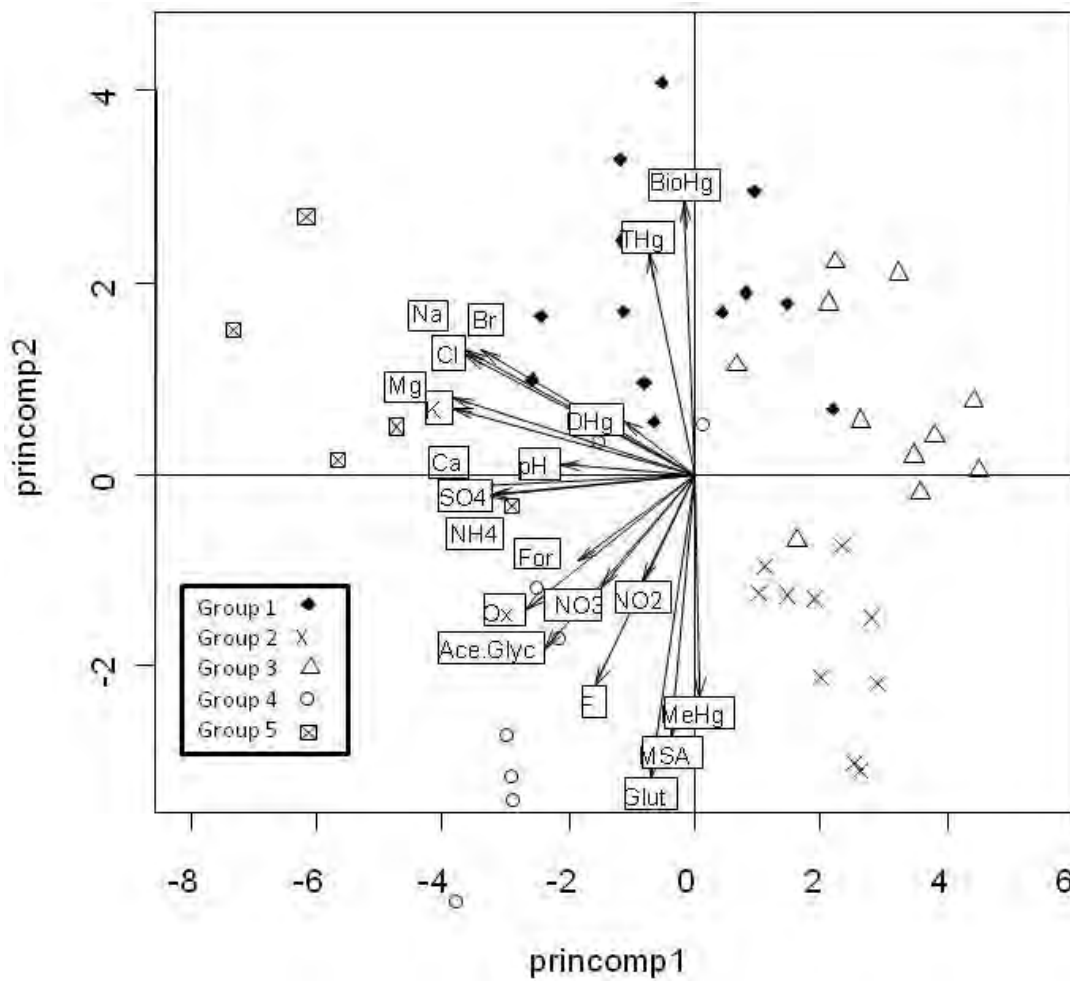
523 Figure 6: Sulfur cycle (modified from Bentley and Chasteen (2004)). The pathways represented here  
524 focus on biogenic transformations and the numbered pathways represent those discussed in the  
525 text. Other transformations occur but are not addressed in this paper. The pathways are: 1) DMSP-  
526 lyase. 2) Demethylation. 3) MMPA demethylation. 4) Thiol transmethylation. 5) Thiol  
527 transmethylation. The star symbol represents reactions where BioHg could potentially be methylated  
528 through methyltransfer reactions.

529

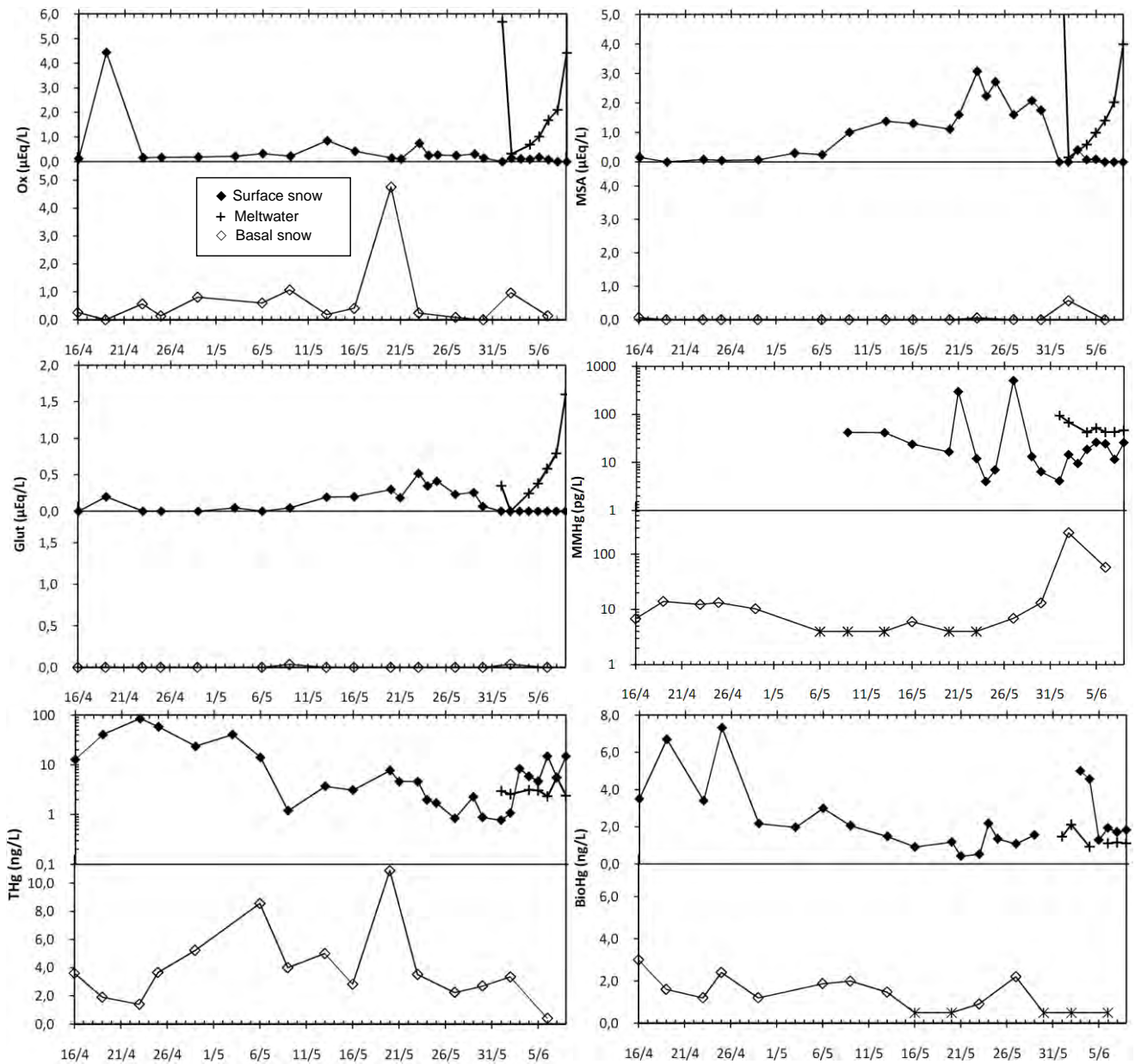




538  
539



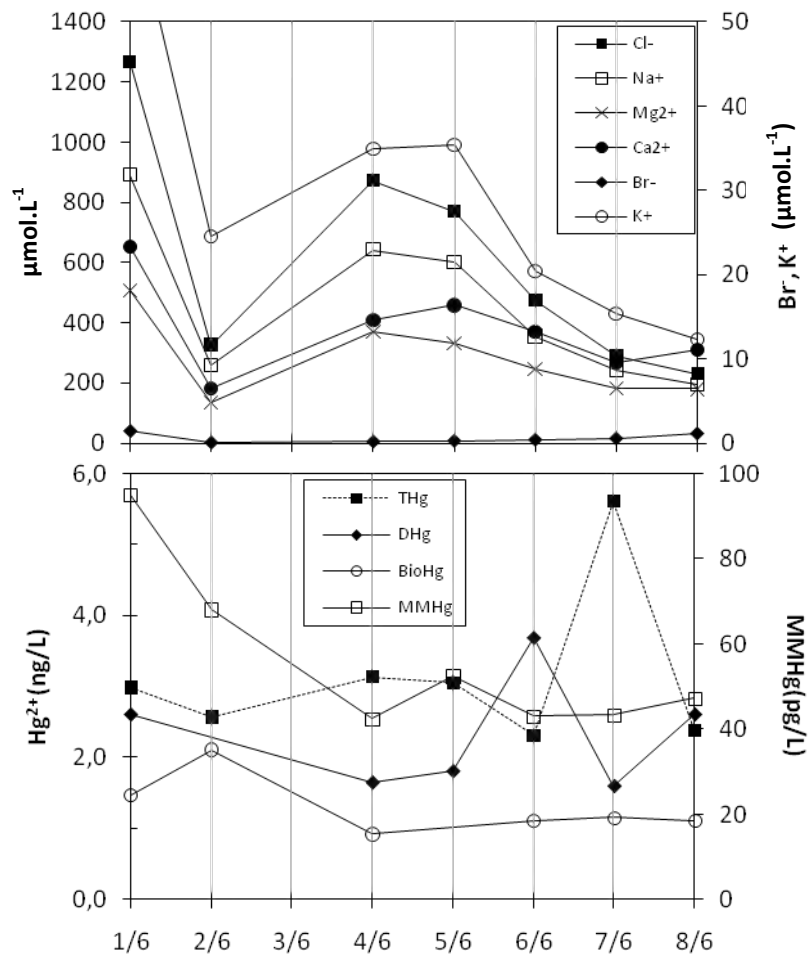
540  
541 Figure 2: Principal component analysis for the sampling period. Chemical data ( $\mu\text{mol.L}^{-1}$  or  $\text{ng.L}^{-1}$  for  
542 Hg species) were log-transformed prior to analysis. The data set covers the entire sampling period  
543 (16<sup>th</sup> April- June 8<sup>th</sup>). Abbreviations: Glut=glutaric acid, MSA=methanesulfonic acid, Ox=oxalic acid,  
544 For=formate, F=fluoride, Ace.Glyc=acetate-glycolate, BioHg=bioavailable Hg, THg=total Hg,  
545 MeHg=methylmercury, DHg=dissolved total Hg  
546



547  
548  
549  
550  
551  
552  
553  
554  
555  
556  
557  
558  
559

Figure 3: Chemical profiles over time for organics (MSA, glutaric acid, oxalic acid) and different mercury species. Organic concentrations are expressed in  $\mu\text{mol.L}^{-1}$ , total mercury (THg) and bioavailable mercury (BioHg) are expressed in  $\text{ng.L}^{-1}$ . Monomethylmercury (MMHg) concentrations are expressed in  $\text{pg.L}^{-1}$ . Full squares represent surface samples, open squares represent basal samples and crosses are meltwater samples. Surface samples for MMHg and HgT are presented on a log-scale. All analyses were carried out in duplicate or triplicate and standard error was less than 10%.

560

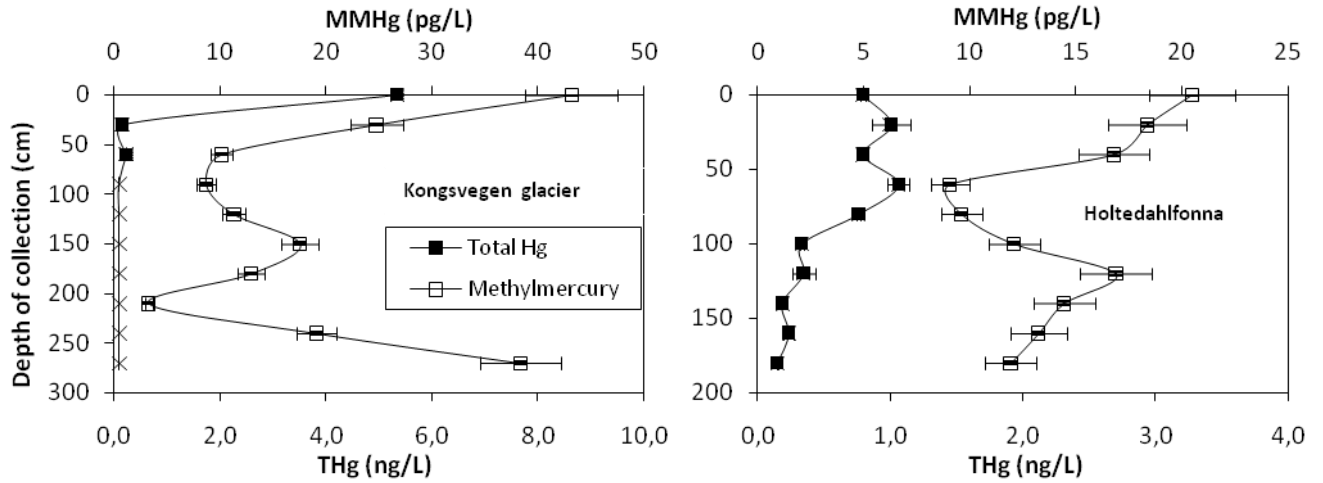


561

562 Figure 4: Meltwater elution curves for major ions and different mercury species over time. Ion  
 563 concentrations are expressed in  $\mu\text{mol.L}^{-1}$ , total (THg), dissolved total (DHg) and bioavailable (BioHg)  
 564 mercury concentrations are expressed in  $\text{ng.L}^{-1}$ . Methylmercury (MMHg) concentrations are in  $\text{pg.L}^{-1}$ .  
 565 Analyses were carried out in duplicate or triplicate and standard error was less than 10%.

566  
 567

568



569  
570  
571  
572  
573  
574  
575

Figure 5: Snowpit total mercury (THg) and monomethylmercury (MMHg) profiles for Holvedahlfonna (sample date 30/04/2008) and Kongsvegen (sample date 19/05/2008) glaciers. ▲



587

588

## REFERENCES

- 589 AMAP, 2009. AMAP Assessment 2009: Human Health in the Arctic. Arctic Monitoring and Assessment  
590 Programme (AMAP), Oslo, Norway.
- 591 Amato P., Hennebelle R., Magand O., Sancelme M., Delort A. M., Barbante C., Boutron C., and Ferrari  
592 C. (2007) Bacterial characterization of the snow cover at Spitzberg, Svalbard. *FEMS Microbiol.*  
593 *Ecol.* **59**, 255-264.
- 594 Ariya P. A., Khalizov A., and Gidas A. (2002) Reactions of gaseous mercury with atomic and molecular  
595 halogens: Kinetics, product studies, and atmospheric implications. *J. Phys. Chem. A* **106**,  
596 7310-7320.
- 597 Bales R. C., Davis R. E., and Williams M. W. (1993) Tracer release in melting snow: diurnal and  
598 seasonal patterns. *Hydrolog. Process.* **7**, 389-401.
- 599 Barkay T., Gillman M., and Turner R. R. (1997) Effects of dissolved organic carbon and salinity on  
600 bioavailability of mercury. *Appl. Environ. Microbiol.* **63**, 4267-71.
- 601 Barkay T. and Poulain A. J. (2007) Mercury (micro)biogeochemistry in polar environments. *FEMS*  
602 *Microbiol. Ecol.* **59**, 232-41.
- 603 Bentley R. and Chasteen T. G. (2004) Environmental VOSCs--formation and degradation of dimethyl  
604 sulfide, methanethiol and related materials. *Chemosphere* **55**, 291-317.
- 605 Berman M., Chase T., Jr., and Bartha R. (1990) Carbon Flow in Mercury Biomethylation by  
606 *Desulfovibrio desulfuricans*. *Appl. Environ. Microbiol.* **56**, 298-300.
- 607 Brooks S., Lindberg S., Southworth G., and Arimoto R. (2008) Springtime atmospheric mercury  
608 speciation in the McMurdo, Antarctica coastal region. *Atmos. Environ.* **42**, 2885-2893.
- 609 Campbell L. M., Norstrom R. J., Hobson K. A., Muir D. C. G., Backus S., and Fisk A. T. (2005) Mercury  
610 and other trace elements in a pelagic Arctic marine food web (Northwater Polynya, Baffin  
611 Bay). *Sci. Total Environ.* **351**, 247-263.
- 612 Celio V., Lean D. R., and Scott S. L. (2006) Abiotic methylation of mercury in the aquatic environment.  
613 *Sci. Total Environ.* **368**, 126-37.
- 614 Choi S. C., Chase Jr. T., and Bartha R. (1994) Enzymatic catalysis of mercury methylation by  
615 *Desulfovibrio desulfuricans* LS. . *Appl. Environ. Microbiol.* **60** 1342-1346.
- 616 Christner B. C. (2002) Incorporation of DNA and protein precursors into macromolecules by bacteria  
617 at -15 degrees C. *Appl. Environ. Microbiol.* **68**, 6435-8.
- 618 Colbeck S. C. (1981) A simulation of the enrichment of atmospheric pollutants in snow cover runoff.  
619 *Water Resour. Res.* **17** 1383-1388.
- 620 Colbeck S. C. (1989) Air movement in snow due to windpumping. *J Glaciol* **35**, 209-213.
- 621 Compeau G. C. and Bartha R. (1985) Sulfate reducing bacteria: principal methylators of mercury in  
622 anoxic estuarine sediment. *Appl. Environ. Microbiol.* **50**, 498-502.
- 623 Constant P., Poissant L., Villemur R., Yumvihoze E., and Lean D. (2007) Fate of inorganic mercury and  
624 methyl mercury within the snow cover in the low arctic tundra on the shore of Hudson Bay  
625 (Québec, Canada). *J. Geophys. Res.* **112**.
- 626 Cossa D., Averty B., and Pirrone N. (2009) The origin of methylmercury in open Mediterranean  
627 waters. *Limnol. Oceanogr.* **54**, 837-844.
- 628 Daly G. L. and Wania F. (2004) Simulating the Influence of Snow on the Fate of Organic Compounds.  
629 *Environ. Sci. Technol.* **38**, 4176-4186.
- 630 Davies T. D., Vincent C. E., and Brimblecombe P. (1982) Preferential elution of strong acids from a  
631 Norwegian ice cap. *Nature* **300**, 161-163.
- 632 Dommergue A., Ferrari C. P., Poissant L., Gauchard P. A., and Boutron C. F. (2003) Diurnal cycles of  
633 gaseous mercury within the snowpack at Kuujuarapik/Whapmagoostui, Quebec, Canada.  
634 *Environ. Sci. Technol.* **37**, 3289-97.

635 Dommergue A., Larose C., Faïn X., Clarisse O., Foucher D., Hintelmann H., Schneider D., and Ferrari C.  
636 P. (2010) Deposition of mercury species in the Ny-Ålesund area (79°N) and their transfer  
637 during snowmelt. *Environ. Sci. Technol.* **44**, 901-907

638 Douglas T. A. and Sturm M. (2004) Arctic haze, mercury and the chemical composition of snow across  
639 northwestern Alaska. *Atmos. Environ.* **38**, 805-820.

640 Edwards A. C., Scalenghe R., and Freppaz M. (2007) Changes in the seasonal snow cover of alpine  
641 regions and its effect on soil processes: A review. *Quatern. Int.* **162–163** 172–181.

642 Eichler A., Schwikowski M., and Gäggeler H. W. (2001) Meltwater induced relocation of chemical  
643 species in Alpine firn. *Tellus* **53B**, 192–203.

644 Ferrari C. P., Moreau A. L., and Boutron C. F. (2000) Clean conditions for the determination of ultra-  
645 low levels of mercury in ice and snow samples. *Fresen. J. Anal. Chem.* **366**, 433–437.

646 Fitzgerald W. F., Lamborg C. H., and Hammerschmidt C. R. (2007) Marine Biogeochemical Cycling of  
647 Mercury. *Chem. Rev.* **107**, 641-662.

648 Fleming E. J., Mack E. E., Green P. G., and Nelson D. C. (2006) Mercury Methylation from Unexpected  
649 Sources: Molybdate-Inhibited Freshwater Sediments and an Iron-Reducing Bacterium. *Appl.*  
650 *Environ. Microbiol.* **72**, 457-464.

651 Gardfeldt K., Munthe J., Stromberg D., and Lindqvist O. (2003) A kinetic study on the abiotic  
652 methylation of divalent mercury in the aqueous phase. *Sci. Total Environ.* **304**, 127-136.

653 Goto-Azuma K., Nakawo M., Han J., Watanabe O., and Azuma N. (1994) Melt-induced relocation of  
654 ions in glaciers and in a seasonal snowpack *IAHS Publ.* **223** 287–298.

655 Grannas A. M., Bausch A. R., and Mahanna K. M. (2007a) Enhanced aqueous photochemical reaction  
656 rates after freezing. *J. Phys. Chem. A* **111**, 11043-9.

657 Grannas A. M., Jones A. E., Dibb J., Ammann M., Anastasio C., Beine H. J., Bergin M., Bottenheim J.,  
658 Boxe C. S., Carver G., Chen G., Crawford J. H., Dominé F., Frey M. M., Guzman M. I., Heard D.  
659 E., Helmig D., Hoffmann M. R., Honrath R. E., Huey L. G., Hutterli M., Jacobi H. W., Klan P.,  
660 Lefer B., McConnell J., Plane J., Sander R., Savarino J., Shepson P. B., Simpson W. R., Sodeau J.  
661 R., von Glasow R., Weller R., Wolff E. W., and Zhu T. (2007b) An overview of snow  
662 photochemistry: evidence, mechanisms and impacts. *Atmos. Chem. Phys.* **7**, 4329-4373.

663 Hall B., Bloom N. S., and Munthe J. (1995) An experimental study of two potential methylation agents  
664 of mercury in the atmosphere: CH<sub>3</sub>I and DMS. *Water Air Soil Pollut.* **80**, 337-341.

665 Hammerschmidt C. R., Lamborg C. H., and Fitzgerald W. F. (2007) Aqueous phase methylation as a  
666 potential source of methylmercury in wet deposition. *Atmos. Environ.* **41**, 1663-1668.

667 Hinkler J., Hansen B. U., Tamstorf M. P., Sigsgaard C., and Petersen D. (2008) Snow and Snow-Cover  
668 in Central Northeast Greenland. *Adv. Ecol. Res.* **40**, 175-195.

669 Hodgkins R., Tranter, M., and Dowdeswell, J. A. (1998) The hydrochemistry of runoff from a  
670 'coldbased' glacier in the High Arctic (Scott Turnerbreen, Svalbard) *Hydrol. Process.* **12**, 87–  
671 103.

672 Johannessen M. and Henriksen A. (1978) Chemistry of snow melt water: changes in concentration  
673 during melting *Water Resour. Res.* **14**, 615-619.

674 Johnson K. P., Blum J. D., Keeler G. J., and Douglas T. A. (2008) Investigation of the deposition and  
675 emission of mercury in arctic snow during an atmospheric mercury depletion event. *J.*  
676 *Geophys. Res.* **113**, doi:10.1029/2008JD009893.

677 Jones H. G. (1999) The ecology of snow-covered systems: a brief overview of nutrient cycling and life  
678 in the cold. *Hydrol Process* **13**, 2135–2147.

679 Kawamura K. and Ikushima K. (1993) Seasonal changes in the distribution of dicarboxylic acids in the  
680 urban atmosphere. *Envir. Sci. Technol.* **27**, 2227-2235.

681 Kawamura K. and Kasukabe H. (1996) Sources and reaction pathways of dicarboxylic acids, ketoacids  
682 and dicarbonyls in Arctic aerosols: one year of observations. *Atmos. Environ.* **30**, 1709-1722.

683 Kerin E. J., Gilmour C. C., Roden E., Suzuki M. T., Coates J. D., and Mason R. P. (2006) Mercury  
684 Methylation by Dissimilatory Iron-Reducing Bacteria. *Appl. Environ. Microbiol.* **72**, 7919-7921.



- 685 Kiene R. P., Linn L. J., and Bruton J. A. (2000) New and important roles for DMSP in marine microbial  
686 communities. *J. Sea Res.* **43**, 209-224.
- 687 Kirk J. L., St. Louis V. L., Hintelmann H., Lehnher I., Else B., and Poissant L. (2008) Methylated  
688 Mercury Species in Marine Waters of the Canadian High and Sub Arctic. *Environ. Sci. Technol.*  
689 **42**, 8367-8373.
- 690 Kirk J. L., St. Louis V. L., and Sharp M. J. (2006) Rapid Reduction and Reemission of Mercury Deposited  
691 into Snowpacks during Atmospheric Mercury Depletion Events at Churchill, Manitoba,  
692 Canada. *Environ. Sci. Technol.* **40**, 7590-7596.
- 693 Kuhn M. (1987) Micro-meteorological conditions for snow melt *J Glaciol* **33**, 24-26.
- 694 Kuhn M. (2001) The nutrient cycle through snow and ice, a review. *Aqua. Sci.* **63**, 150-167.
- 695 Lalonde J. D., Poulain A. J., and Amyot M. (2002) The role of mercury redox reactions in snow on  
696 snow-to-air mercury transfer. *Environ. Sci. Technol.* **36**, 174-178.
- 697 ~~Larose C., Dommergue A., Ferrari C., Maruszczak N., Coves J., and Schneider D. (2010) Detection of~~  
698 ~~bioavailable Hg deposited in Polar regions. *The ISME Journal* submitted.~~
- 699 Leck C. and Persson C. (1996) The central Arctic Ocean as a source of dimethyl sulfide - Seasonal  
700 variability in relation to biological activity *Tellus* **48B**, 156-177.
- 701 Legrand M., Preunkert S., Oliveira T., Pio C. A., Hammer S., Gelencsér A., Kasper-Giebl A., and Laj P.  
702 (2007) Origin of C2-C5 dicarboxylic acids in the European atmosphere inferred from year-  
703 round aerosol study conducted at a west-east transect. *J. Geophys. Res.* **112**, D23S07,  
704 doi:10.1029/2006JD008019.
- 705 Lei Y. D., D. Y., and Wania F. (2004) Is rain or snow a more efficient scavenger of organic chemicals?  
706 *Atmos. Environ.* **38**, 3557-3571.
- 707 Lindberg S. E., Brooks S., Lin C. J., Scott K., Meyers T., Chambers L., Landis M., and Stevens R. (2001)  
708 Formation of Reactive Gaseous Mercury in the Arctic: Evidence of Oxidation of Hg<sup>0</sup> to Gas-  
709 Phase Hg-III Compounds after Arctic Sunrise. *Water Air Soil Poll. Focus* **1**, 295-302.
- 710 Lindberg S. E., Brooks S., Lin C. J., Scott K. J., Landis M. S., Stevens R. K., Goodsite M., and Richter A.  
711 (2002) Dynamic Oxidation of Gaseous Mercury in the Arctic Troposphere at Polar Sunrise.  
712 *Environ. Sci. Technol.* **36**, 1245-256.
- 713 Loseto L. L., Lean D. R. S., and Siciliano S. D. (2004) Snowmelt Sources of Methylmercury to High  
714 Arctic Ecosystems. *Environ. Sci. Technol.* **38**, 3004-3010.
- 715 Lu J. Y., Schroeder W. H., Barrie L. A., Steffen A., Welch H. E., Martin K., Lockhart L., Hunt R. V., Boila  
716 G., and Richter A. (2001) Magnification of atmospheric mercury deposition to polar regions in  
717 springtime: the link to tropospheric ozone depletion chemistry. *Geophys. Res. Lett.* **28**, 3219-  
718 3222.
- 719 Lyons W. B., Welch K. A., Fountain A. G., Dana G. L., Vaughn B. H., and McKnight D. M. (2003) Surface  
720 glaciochemistry of Taylor Valley, southern Victoria Land, Antarctica, and its relation to stream  
721 chemistry. *Hydrolog. Process.* **17** 115-130.
- 722 Meyer T., Lei Y. D., and Wania F. (2006) Measuring the release of organic contaminants from melting  
723 snow under controlled conditions. *Environ. Sci. Technol.* **40**, 3320-3326.
- 724 Meyer T. and Wania F. (2008) Organic contaminant amplification during snowmelt. *Water Res.* **42**,  
725 1847-1865.
- 726 Monperrus M., Tessier E., Amouroux D., Leynaert A., Huonnic P., and Donard O. F. X. (2007) Mercury  
727 methylation, demethylation and reduction rates in coastal and marine surface waters of the  
728 Mediterranean Sea. *Mar. Chem.* **107**, 49-63.
- 729 Narcy F., Gasparini S., Falk-Petersen S., and Mayzaud P. (2009) Seasonal and individual variability of  
730 lipid reserves in *Oithona similis* (Cyclopoida) in an Arctic fjord. *Polar Biol.* **32**, 233-242.
- 731 Niki H., Maker P. D., Savage C. M., and Breitenbach L. P. (1983a) A long-path Fourier transform  
732 infrared study of the kinetics and mechanism for the hydroxyl radical-initiated oxidation of  
733 dimethylmercury. *J. Phys. Chem.* **87**, 4978 - 4981.

734 Niki H., Maker P. S., Savage C. M., and Breitenbach L. P. (1983b) A Fourier-transform infrared study of  
735 the kinetics and mechanism of the reaction of atomic chlorine with dimethylmercury. *J. Phys.*  
736 *Chem.* **87**, 3722-3724.

737 Poulain A. J., Lalonde J. D., Amyot M., Shead J. A., Raofie F., and Ariya P. A. (2004) Redox  
738 transformations of mercury in an Arctic snowpack at springtime. *Atmos. Environ.* **38**, 6763-  
739 6774.

740 Poulain A. J., Ni Chadhain S. M., Ariya P. A., Amyot M., Garcia E., Campbell P. G. C., Zylstra G. J., and  
741 Barkay T. (2007) Potential for mercury reduction by microbes in the high arctic. *Appl. Environ.*  
742 *Microbiol.* **73**, 2230-2238.

743 Reisch C. R., Moran M. A., and Whitman W. B. (2008) Dimethylsulfoniopropionate-dependent  
744 demethylase (DmdA) from *Pelagibacter ubique* and *Silicibacter pomeroyi*. *J. Bacteriol.* **190**,  
745 8018-24.

746 Rontani J.-F. (2001) Visible light-dependent degradation of lipidic phytoplanktonic components  
747 during senescence: a review. *Phytochemistry* **58**, 187-202.

748 Schroeder W. H., Anlauf K. G., Barrie L. A., Lu J. Y., Steffen A., Schneeberger D. R., and Berg T. (1998)  
749 Arctic springtime depletion of mercury. *Nature* **394**, 331-332.

750 Scott K. J. (2001) Bioavailable mercury in arctic snow determined by a light-emitting mer-lux  
751 bioreporter. *Arctic* **54**, 92-95.

752 Siciliano S. D., O'Driscoll N. J., Tordon R., Hill J., Beauchamp S., and Lean D. R. S. (2005) Abiotic  
753 production of methylmercury by solar radiation. *Environ. Sci. Technol.* **39**, 1071-1077.

754 St. Louis V. L., Hintelmann H., Graydon J. A., Kirk J. L., Barker J., Dimock B., Sharp M. J., and Lehnher  
755 I. (2007) Methylated mercury species in Canadian high arctic marine surface waters and  
756 snowpacks. *Environ. Sci. Technol.* **41**, 6433-6441.

757 St. Louis V. L., Sharp M. J., Steffen A., May A., Barker J., Kirk J. L., Kelly D. J. A., Arnott S. E., Keatley B.,  
758 and Smol J. P. (2005) Some sources and sinks of monomethyl and inorganic mercury on  
759 Ellesmere island in the Canadian high arctic. *Environ. Sci. Technol.* **39**, 2686-2701.

760 Stoichev T., Rodriguez Martin-Doimeadios R. C., Tessier E., Amouroux D., and Donard O. F. (2004)  
761 Improvement of analytical performances for mercury speciation by on-line derivatization,  
762 cryofocussing and atomic fluorescence spectrometry. *Talanta* **62**, 433-8.

763 Sunderland E. M., Krabbenhoft D. P., Moreau J. W., Strode S. A., and Landing W. M. (2009) Mercury  
764 sources, distribution, and bioavailability in the North Pacific Ocean: Insights from data and  
765 models. *Global Biogeochem. Cycles* **23**.

766 Tranter M., Brimblecombe P., Davies T. D., Vincent C. E., Abrahams P. W., and Blackwood I. (1986) A  
767 composition of snowfall, snowpack and meltwater in the Scottish Highlands—evidence for  
768 preferential elution *Atmos. Environ.* **20**, 517-525.

769 Tseng C. M., Garraud H., Amouroux D., Donard O. F., and de Diego A. (1998) Open focused  
770 microwave-assisted sample preparation for rapid total and mercury species determination in  
771 environmental solid samples. *J. Autom. Chem.* **20**, 99-108.

772 Wagemann R., Trebacz E., Boila G., and Lockhart W. L. (1998) Methylmercury and total mercury in  
773 tissues of arctic marine mammals. *Sci. Total Environ.* **218**, 19-31.

774 Weber J. H. (1993) Review of possible paths for abiotic methylation of mercury(II) in the aquatic  
775 environment. *Chemosphere* **26**, 2063-2077.

776 Williams M. W., Seibold C., and Chowanski K. (2009) Storage and release of solutes from a subalpine  
777 seasonal snowpack: soil and stream water response, Niwot Ridge, Colorado. *Biogeochemistry*  
778 **95**, 77-94.

779  
780